

# Integration of solar and wind energy systems with PI and PID controller

Suresh Kumar Tummala<sup>1\*</sup>, Rakesh G<sup>1</sup>, Ibrahim H. Al-Kharsan<sup>2,3</sup>, Praveen Kumar Shah<sup>4</sup>

<sup>1</sup> Department of Electrical & Electronics Engineering, Gokaraju Rangaraju Institute of Engineering & Technology, Hyderabad, Telangana, 500090 INDIA

<sup>2</sup> Computer Technical Engineering Department, College of Technical Engineering, The Islamic University, Najaf, Iraq

<sup>3</sup> Department of Electrical Engineering, Faculty of Engineering, University of Kufa, Najaf, 54001, Iraq

<sup>4</sup> Uttaranchal School of Computing Sciences, Uttaranchal University, Dehradun 248007 INDIA

**Abstract.** Because of the rising worry about global warming and the depletion of fossil fuel supplies, many individuals are looking into sustainable energy alternatives to protect the environment for future generations. Because of the situation of our deteriorating globe, eco-friendly items are more in demand than ever. The outcomes of using PI and PID controllers in solar and wind integration are compared in this research. This investigation contains a boost converter, an inverter, a converter, and three induction motors. Wind and solar energy are transformed to DC voltage, then to AC voltage via an inverter, and ultimately to a three-phase induction motor. The boost converter receives output from the wind energy conversion system (WECS). The solar output is routed to the three-phase complete converter. Sinusoidal pulse width modulation used in generating trigger pulses to the inverter. The output of the boost converter is fed into the common dc link by the three phase Sinusoidal pulse width modulation (SPWM) inverter, which converts its dc input to three phase AC output. This system's behaviour is examined using MATLAB Simulink.

Keywords

Inverter, three phase full converter, Boost converter, sinusoidal pulse width modulation, PI controller, PID controller.

## Nomenclature

ABRIVATION	EXPLANATIOIN
Vwind	Voltage at the input of the three phase full converter (Voltage from wind)
Vsolar	Voltage at the input of the boost converter

\* Corresponding author: sureshkumar255@gmail.com

	(Voltage from solar plates)
Vabc	Voltage at the input of the induction motor
Iwind	Current at the input of the three-phase full converter (Current from wind)
Isolar	Current at the input of the boost converter (Current from solar)
Iabc	Current at the input of the induction motor
Vdc	Voltage at the input inverter
Nset	Required speed
N	Actual speed of induction motor

## 1 Introduction

Fossil fuels are becoming increasingly scarce throughout the planet, posing a serious hazard [1]. Most of the power demand is now fulfilled by nuclear power plants and fossil fuels, with a smaller fraction relying on renewable energy sources such as solar, wind, geothermal, and biomass. Solar and wind energy consumption has been quickly expanding in the last ten years [2], therefore renewable energy sources have received more attention and progress in utilisation systems and energy conversion has occurred. The main aims of these advancements are energy conversion, environmental harm reduction, and better safety. Renewable energy can be sent directly to isolated loads or to the grid [3]. Standalone system has huge applications example for small area electrification, supply to isolated area and ware pumps.in renewable energy systems pv and wind are most promising.[4]

Renewable energy utilisation in power systems is expanding, particularly wind and solar photovoltaic systems [5]. Renewable energy accounted for around 19% of total energy consumption in 2012, and this figure is expected to rise in 2013 according to 2014 reports [1]. Solar energy is energy derived from the sun. It is unlimited, renewable, and pollution-free. A solar-charged battery system can provide 24-hour electricity regardless of weather conditions, and enormous amounts of power can be recovered by maintaining some proper technologies [6]. PV array, chopper, inverter, and load are the components of solar PV. To operate power converters and optimise the performance of a PV system, an appropriate algorithm is required. The duty cycle of the chopper may be changed, and by doing so, the most power can be extracted. Inverters are used to transform dc power from a chopper into required alternating current power at the desired frequency and voltage [7].

Wind energy is derived from the wind's kinetic energy. Wind kinetic energy is turned into electrical energy [8]. Wind power is the most competitive renewable technology; industrialised countries have incredible wind resources, both onshore and offshore. Onshore generation can compete with fossil-fuel-fired electricity [9]. It has risen during the last decade. It is both ecologically benign and typically more cost effective than traditional power generating. Wind energy systems create alternating current (AC), which has varying frequencies and voltage levels due to variable speed operation. Solar PV creates direct current voltage, which varies due to sun irradiation and temperature. Power electronic interface is required to connect these two energy systems. [4]

Integration of energy systems and renewable sources in power electronic technologies [5]. The finest hybrid combination of renewable energy sources is standalone solar and wind. It also considers seasonal variations [10]. During the monsoon, wind produces more power and solar produces less. Solar generates more electricity in the summer, but wind generates less, therefore the two are complementing [11]. Wind and solar are linked to rectifier and

boost converters, respectively, and the output is connected and supplies DC as the input to the inverter, and the inverter provides power to the load, in this case an induction motor. MATLAB SIMULINK is used to simulate and analyse the system's behaviour.

## 2 Proposed system

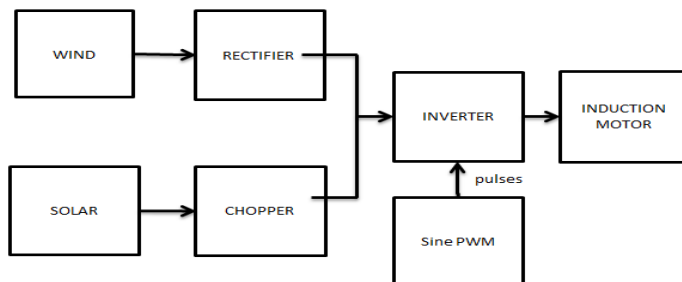
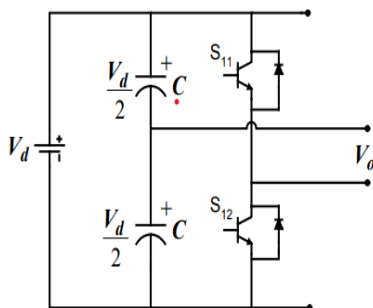


**Fig. 1.** Block diagram

Solar energy is used to power the proposed system, while wind energy is used to power the load. In this system, dc voltage is utilised in lieu of the PV array, and three phase ac with a frequency of 50 Hz is used in place of wind power. In general, a solar system comprises of a PV array, a dc voltage source, and a boost converter. A boost converter raises the voltage. In general, a solar system consists of a wind turbine, however in this case, an alternating current voltage source is employed, as well as a rectifier that converts alternating current to direct current [12]. The output of the rectifier in the wind section and the boost converter in the solar part are linked and fed into the inverter, which converts dc to ac. The load induction motor receives AC electricity from the inverter. The sine PWM generates the pulses for the inverter. PWM, PI, and PID controllers are utilised in sine. The controllers receive a speed error signal, which lowers the difference between the programmed speed and the actual speed of the induction motor [13]. The speed of the induction motor in this system should be like the reference speed.

## 3 Sinusoidal pulse width modulation

Sinusoidal PWM, also known as sub oscillation subharmonic and triangulation, is commonly utilised in industrial applications. With SPWM,  $V_c$  is the magnitude of the triangular carrier wave and  $V_r$  is the magnitude of the reference wave. When the carrier wave and the reference wave meet, these intersections are switching instants.



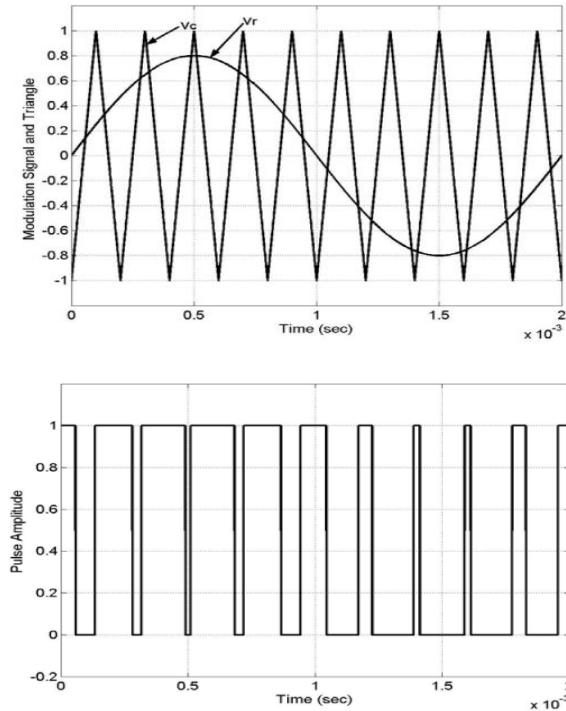


**Fig. 2.** Sinusoidal PWM [4]

PWM scheme is explained in above figure, in this  $V_c$  is the triangular carrier wave and  $V_r$  is the reference signal, inverter in following figure is controlled based on comparison of triangular and reference signal. when reference signal is higher in magnitude than triangular then comparator output is high and reference signal is low compared to the triangular then output is low

$$\begin{aligned}
 V_r > V_c & \quad \text{then} \quad V_{out} = V_d/2 \\
 V_r < V_c & \quad \text{then} \quad V_{out} = -V_d/2
 \end{aligned} \tag{1}$$

The ratio of Reference voltage magnitude to carrier voltage magnitude is called modulation index( $m_i$ ). modulation index controls harmonic content in voltage waveform of output. fundamental component's magnitude of the output waveform is proportional to the modulation index( $m_i$ ).

$$\text{Frequency modulation ratio } m_f \text{ is } M_f = f_i/f_m \tag{2}$$

Two switches on the same leg is not turn on at same time to satisfy Kirchoff's voltage law  $K_i$

$$S_{11} + S_{12} = 1$$

For each inverter, this enables voltage of output to fluctuate from  $-V_d/2$  and  $V_d/2$

### 4 PI Controller used in integration of solar and wind systems

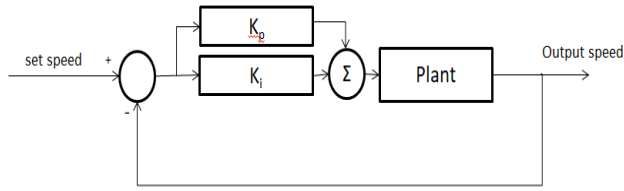


**Fig. 3.** PI controller

Above figure is the pi controller block diagram, by varying the  $K_p$ ,  $K_i$  steady state error can eliminate, remaining errors can predict. pi controller cannot be decrease rise time and oscillations.

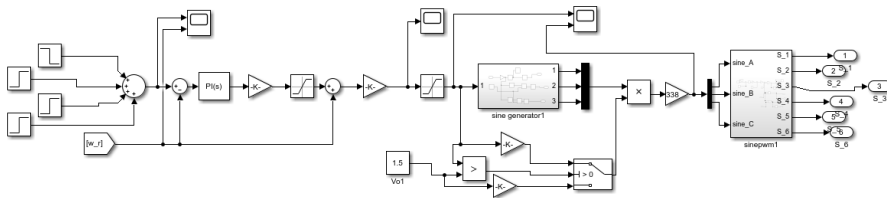


**Fig. 4.** Triggering pulse generation to the inverter while using the pi controller

In solar and wind integration, a PI controller is utilised to regulate the speed of an induction motor. The load connected to the inverter is an induction motor. Peak overrun at 3 seconds is 364.235, with a peak overshoot percentage of 24.685%, peak overshoot at 5 seconds is 441.728, with a peak overshoot percentage of 13.33%, and peak overshoot at 6 seconds is 473.363, with a peak overshoot percentage of 7.93%.

The 4th cycle peak readings are 293.409 (positive peak),286.679 (negative peak) with 3 seconds of reference speed variation (negative peak). The peak-to-peak value is 6.73. At 5 seconds of reference speed change, the 4th cycle peak values are 388.381 (positive peak), 383.816 (negative peak) (negative peak). The peak-to-peak value is 4.565. The 4th cycle peak readings are 436.723 (positive peak),431.982 (negative peak) with 6 seconds of reference speed variation (negative peak). The peak-to-peak value is 4.742.

### 5 PID Controller used in the integration of solar and wind systems

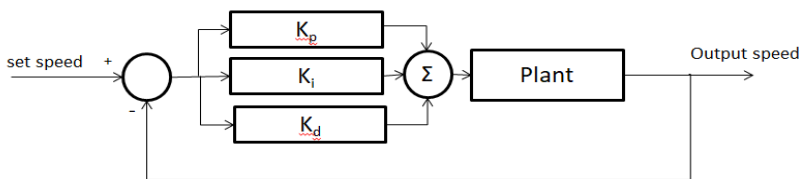


**Fig. 5.** PID controller

PID controller block diagram shown in fig 5.it has characteristics of improve transient response, reduced rise time and no presence of oscillation in output response.it gives higher stability of system.  $K_p$ ,  $K_i$  and  $K_d$  can be adjusted to get required performance in MATLAB SIMULINK. In MATLAB SIULINK gains can be tuned automatically by PID tuner.in frequency response, by varying  $K_p$  rise time can reduced, by varying  $K_i$  steady state error can eliminated, by varying  $K_d$  setting time can be adjusted.

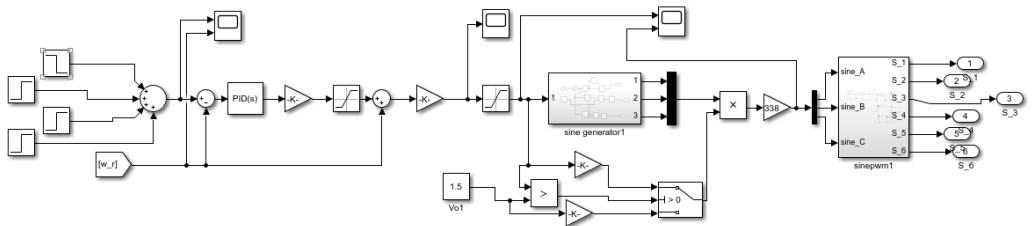


**Fig. 6.** Triggering pulse generation to the inverter while using the PID controller

Peak overrun at 3 seconds is 364.5, with a peak overshoot percentage of 26.031%, highest overshoot at 5 seconds is 438.85, with a peak overreach percentage of 13.765%. The highest overshoot at 6 seconds is 469.696, and the top overrun percentage is 8.219%. The 4th cycle peak readings are 295.622 (positive peak), 289.0802 (negative peak) with 3 seconds of reference speed variation (negative peak). The peak-to-peak value is 6.542. During a 5 second variation in reference speed, the 4th cycle peak values are 392.176 (positive peak), 387.722 (negative peak) (negative peak). The peak-to-peak value is 4.455. The 4th cycle peak values are 441124 (positive peak),436.437 (negative peak) with 6 seconds of reference speed change (negative peak). The peak-to-peak value is 4.687.

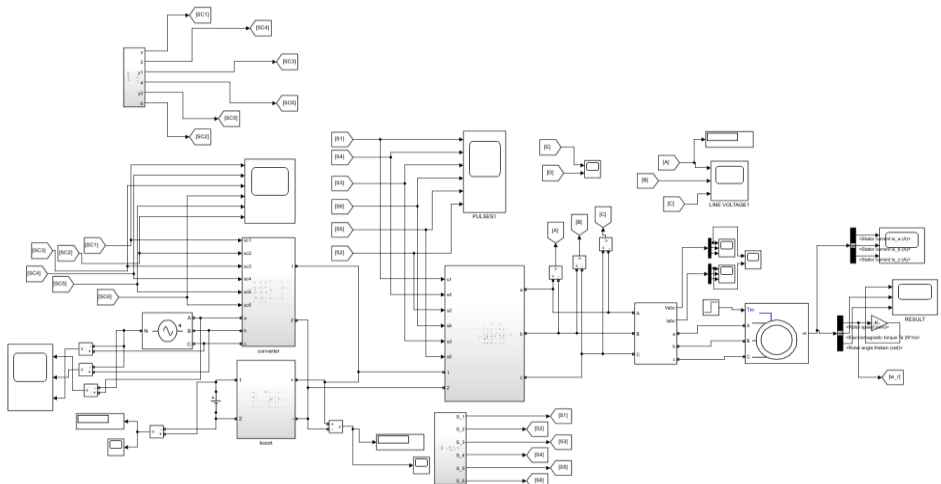


**Fig. 7.** Simulation diagram of the solar and wind integration

## 6 Simulation results

### 6.1 PID controller

After using the pid controller in the system the speed of the system is mentioned below

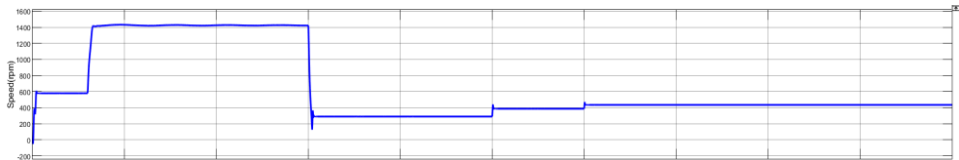


**Fig. 8.** Speed of the induction motor when PID controller is used.

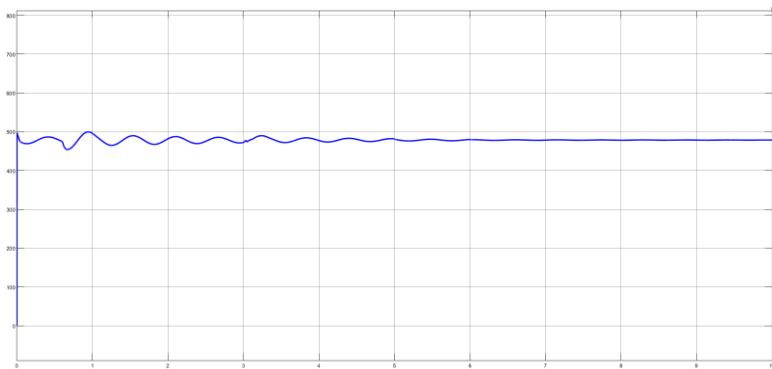


**Fig. 9.** Input voltage at the inverter(Vdc)

Above figure is the voltage signal is given to the inverter, which is the DC link voltage while PID controller is used.

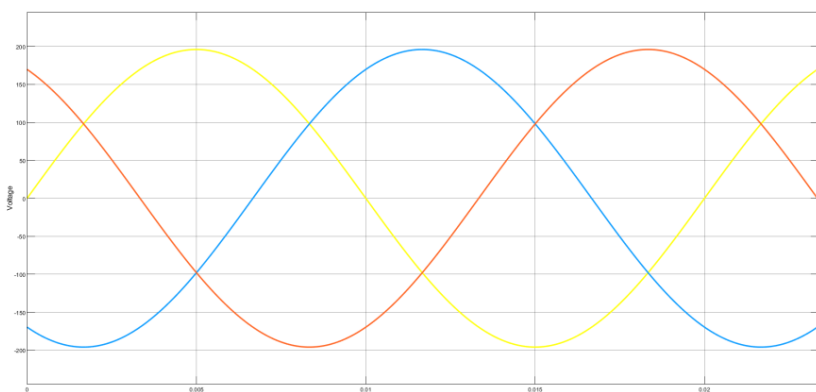


**Fig. 10.** Input voltage of the three-phase full converter

The above figure is about three phase supply is given to three phase fully controlled converter while PID controller is used.

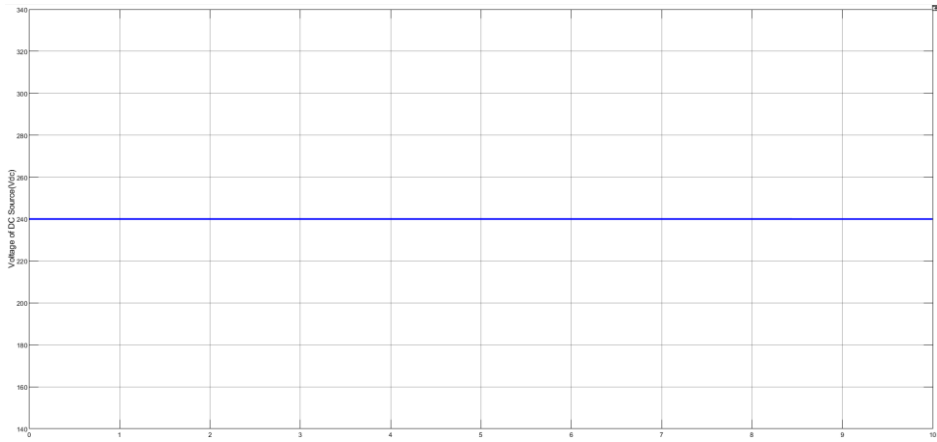


**Fig. 11.** Input voltage at the boost converter

The above figure is about DC supply is given to boost converter while PID controller is used.

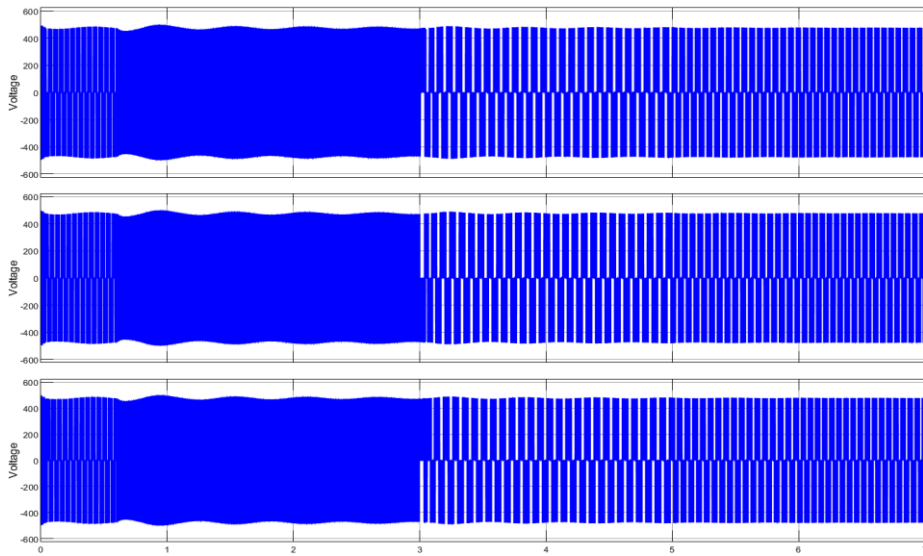


**Fig. 12.** Output Line voltage of the inverter while using PID controller



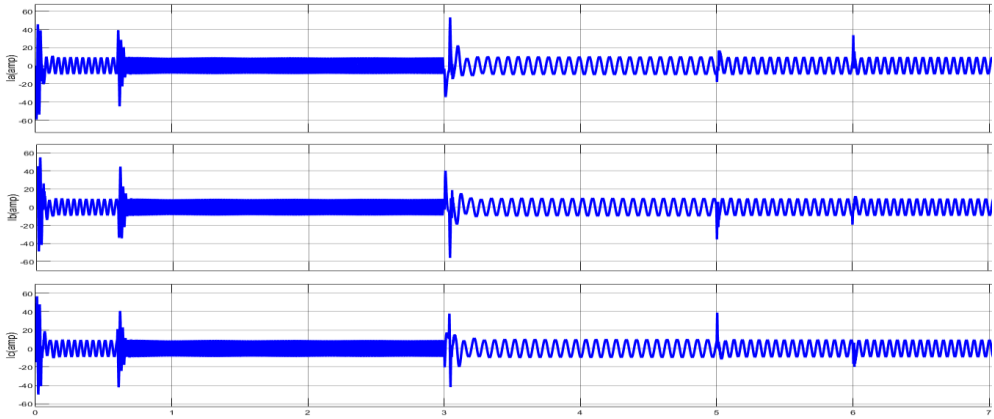


**Fig. 13.** Output current of the inverter while using PID controller

### 6.2 PI controller

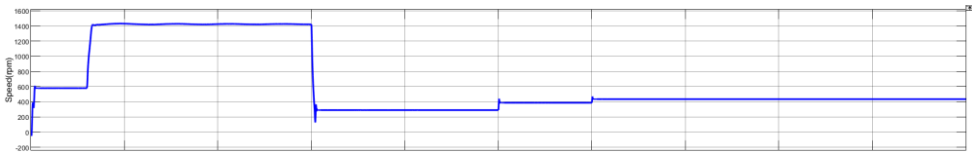


**Fig. 14.** speed of the induction motor when PI controller is used.

Above figure 14 shows the speed of the induction motor when PI controller used in the system

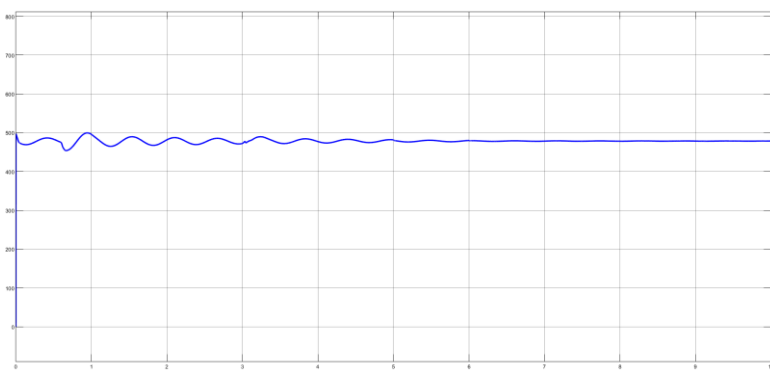


**Fig. 15.** Input voltage at the inverter ( $V_{dc}$ )

Above figure 15 is the voltage signal is given to the inverter, which is the DC link voltage while PI controller is used.

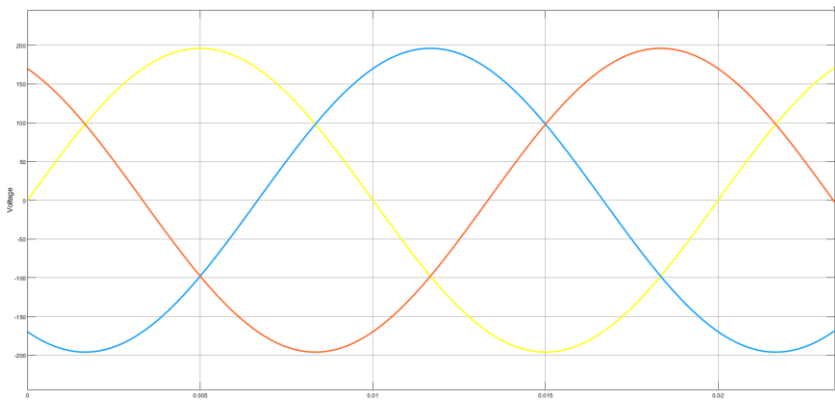


**Fig. 16.** Input voltage of the three-phase full converter

The above figure 16 is about three phase supply is given to three phase fully controlled converter while PI controller is used.

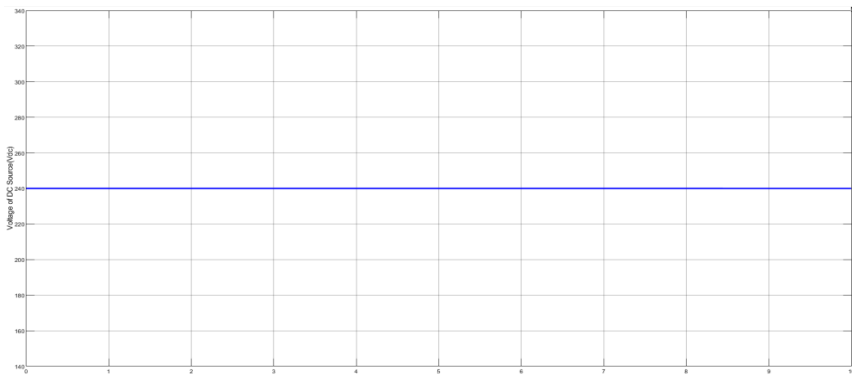


**Fig. 17.** Input voltage at the boost converter

The above figure 17 is about DC supply is given to boost converter while PI controller is used.

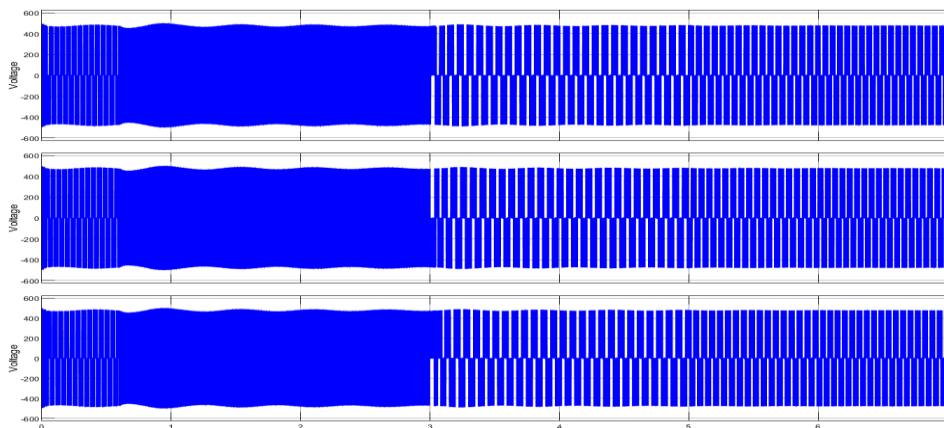


**Fig. 18.** Output Line voltage of the inverter while using PI controller

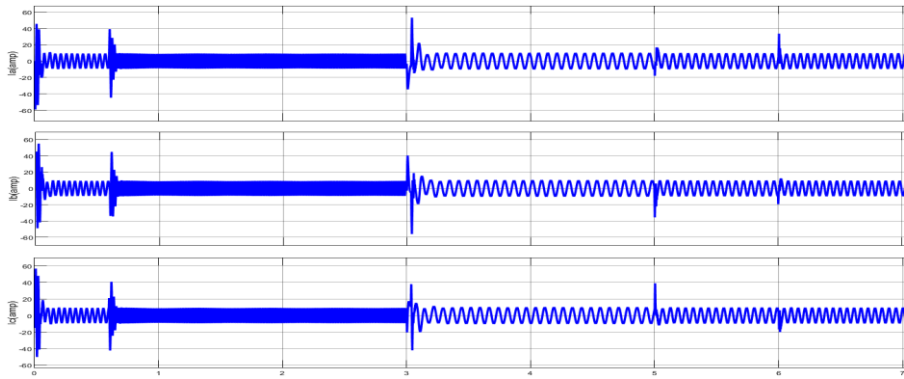


**Fig. 19.** Output current of the inverter while using PI controller

### 6.3 Comparative analysis of PI and PID controllers

These are the findings of comparing the PI and PID controllers in solar and wind integration. For comparison, two criteria are considered: peak overshoot value and peak to peak value. Table 1 compares the peak overshoot of PI and PID controllers, and Table 2 compares the peak-to-peak value of PI and PID controllers.

**Table 1.** Comparison of peak overshoot of PI and PID controllers

Peak overshoot (%)	PI	PID
At 3 <sup>rd</sup> second	26.031%	24.685%
At 5 <sup>th</sup> second	13.765%	13.33%
At 6 <sup>th</sup> second	8.2199%	7.93%

When comparing the peak overshoot at the third second after utilising the PI and PID controllers in solar wind integration, the PID has the less peak overshoot i.e. 24.685%, the PI has the less peak overshoot i.e. 13.33, and the PID has the less peak overshoot i.e. 7.93%. Based on the preceding three examples, the PID controller has a lower peak overshoot value, making it superior to the PI controller.

**Table 2.** Comparison of peak-to-peak value of PI and PID controllers

Peak overshoot (%)	PI	PID
At 3 <sup>rd</sup> second	4.7418	4.6868
At 5 <sup>th</sup> second	4.565	4.455
At 6 <sup>th</sup> second	6.7301	6.542

When comparing the peak overshoot at the 3rd second after utilising the PI and PID controllers in solar wind integration, PID has the less peak to peak value of 4.6868, at the 5th second PID has the less peak to peak value of 4.455, and at the 6th second PID has the less peak overshoot of 6.542. Based on the preceding three examples, the PID controller has a lower peak overshoot value, making it superior to the PI controller.

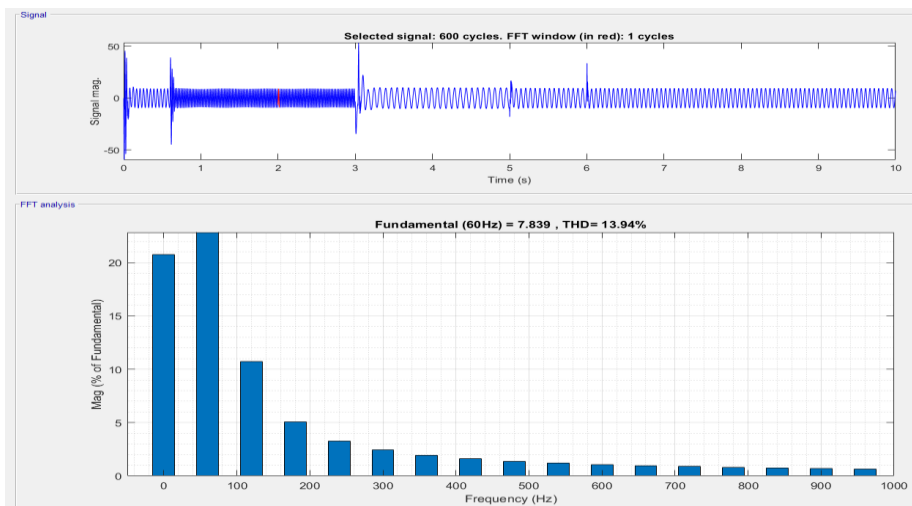


**Fig. 20.** THD value when PI controller is used.

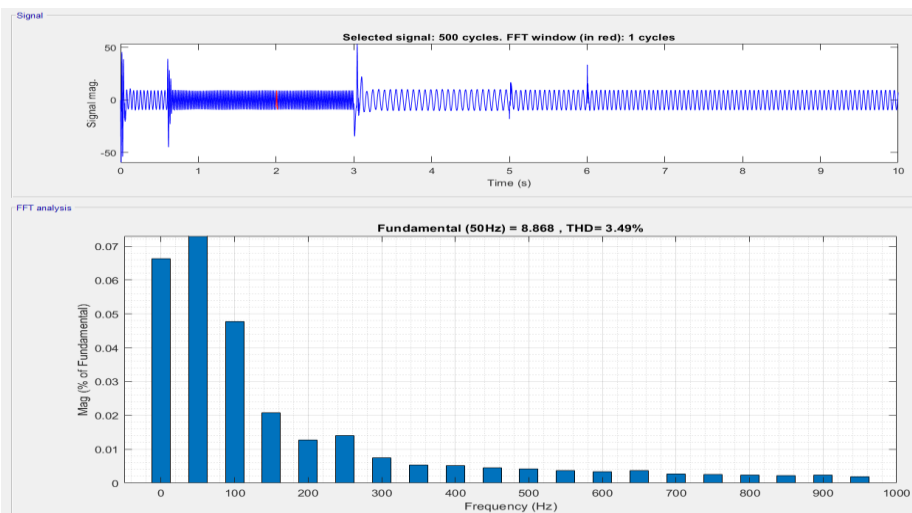


**Fig. 21.** THD value when PID controller is used

THD value of inverter output current when PI controller is used, as shown in fig.20 and 21, is 13.49%, while THD value of inverter output current when PID controller is used in system is 3.49%. As a result of the aforementioned comparison, the PID controller performs better.

## 7 Conclusion

PID outperforms in both the peak overshoot and peak to peak value of speed parameters. In integrating solar and wind power, PI and PID controllers are employed. When comparing the speed of the induction motor, the PID controller will offer a satisfactory response. While comparing the speed, the peak-to-peak value and peak overshoot are taken into account, as well as the settle time, which indicates that the PID controller is producing strong performance. Because the THD value of the input current to the induction motor is 3.49 when the PID controller is used and 13.94% when the PI controller is used, the PID controller will work well. The above study was carried out using a MATLAB simulation.

## References

- 1 M. Brower, E. M. Galán, J. F. Li, D. Green, R. Hinrichsrahlwes, S. Sawyer, M. Sander, R. Taylor, H. Kopetz, and S. Smart Science 134 Gsänger, “Renewables 2014 global status report,” REN21 2014 (2014)
- 2 Rao. J.S., Tummala S.K., Kuthuri, N.R., Nanotechnology for Environmental Engg., **7**, 393-403, (2022)
- 3 Raju, N.A., Suresh Kumar T., Int. Jour. Of Innovative Tech. and Exploring Engg. **8**, 11, 3860-3864 (2019)
- 4 Wai RJ, Lin CY, Chang YR, “Novel maximum power extraction algorithm for PMSG wind generation system”, IET Electr Power Appl,1(2), 275- 283, (2007)
- 5 Karim Mousa, Hamzah AlZu’bi, Ali Diabat, IEEE Xplore, (2010)
- 6 Satyanarayana, K., Gopal, A.V., Babu, P.B., Design optimisation of machining parameters for turning titanium alloys with taguchi-grey method, International Journal of Machining and Machinability of Materials, 2013, 13(2-3), pp. 191–202
- 7 Chandragupta Mauryan.K.S, Nivethitha.T, Yazhini.B, Preethi.B , *IJERA*, **4**, 5(2014)
- 8 Bankupalli P.T., Srikanth Babu V., Suresh Kumar T., Int. Jou. Of Applied Engg. Research., **10**, 16, 37057-37062, (2015)
- 9 Satyanarayana Kosaraju, Swadesh Kumar Singh, Tanya Buddi, Anil Kalluri & Ahsan Ul Haq (2020) Evaluation and characterisation of ASS316L at sub-zero temperature, Advances in Materials and Processing Technologies, 6:2, 365-375
- 10 Tummala S K, Dhasharatha G, *Artificial neural networks based SPWM technique for speed control of permanent magnet synchronous motor*, E3S Web of Conferences, **87**, 01030, (2019)
- 11 J.Godson, M.Karthick, T.Muthukrishnan, M.S.Sivagamasundari *IJAREEIE*, **2**, 11 (2013)
- 12 Satyanarayana, K., Gopal, A.V., Babu, P.B., Design optimisation of machining parameters for turning titanium alloys with taguchi-grey method, International Journal of Machining and Machinability of Materials, 2013, 13(2-3), pp. 191–202
- 13 Davu, S.R., Tejavathu, R. & Tummala, S.K. EDAX analysis of poly crystalline solar cell with silicon nitride coating. Int J Interact Des Manuf (2022).
- 14 Karthik Rao, R., Bobba, P.B., Suresh Kumar, T., Kosaraju, S., Feasibility analysis of different conducting and insulation materials used in laminated busbars, Materials Today: Proceedings, 2019, 26, pp. 3085–3089.
- 15 J. Srinivas Rao, Suresh Kumar Tummala, Narasimha Raju Kuthuri, Comparative investigation of 15 Level and 17 level cascaded h-bridge MLI with cross h-bridge MLI fed permanent magnet synchronous motor, Indonesian Journal of Electrical Engineering and Computer Science, 21(2), pp: 723-734, (2020)
- 16 Nema Parveen, VarshaSharma, IRJET, **5**, 12,Dec 2018.